2023 62nd IEEE Conference on Decision and Control (CDC)
December 13-15, 2023. Marina Bay Sands, Singapore

Adaptive Finite Time Prescribed Performance Fault Tolerant Control for Spacecraft Attitude Maneuver*

Ze Yang[1], Baoqing Yang[1], Ruihang Ji[2] and Jie Ma[1]

Abstract— In this paper, an active fault tolerant control method for spacecraft against actuator faults, uncertainties and disturbances is investigated. First, an adaptive iterative learning observer with improved adaptive law is proposed, which greatly improves the accuracy and speed of fault estimation. Then, a novel adaptive finite time prescribed performance fault tolerant controller is proposed, which has flexible performance constraints according to faults and control references, with better robustness and lower conservatism, breaking the limitation of fixed performance constraint. Next, an online optimal control allocation strategy is designed to achieve high-performance actuator allocation under saturation and fault constraints. Finally, through numerical simulation, the effectiveness and robustness of the proposed scheme are illustrated by comparing with existing methods.

I. INTRODUCTION

In recent years, as the attitude control system (ACS) of spacecraft plays a crucial role in space missions [1], how to deal with non-fatal failures autonomously and efficiently has attracted extensive research [2].

The pursuit of high reliability has led to many methods proposed to achieve fault tolerant control (FTC), which can usually be divided into passive fault tolerant control (PFTC) and active fault tolerant control (AFTC) [3], [4]. The PFTC consists of fixed controllers, which has low complexity, but is conservative in terms of performance [5]. By contrast, AFTC needs to design the fault diagnosis (FD) module and reconfigure the controller according to the real-time diagnosis results, which has optimal performance, higher flexibility [6]. But the accuracy and speed of FD directly determine the control performance, so more efficient FD methods are needed.

FD methods mainly include extended state observer [7], Kalman filter [8], iterative learning observer (ILO) [9], sliding mode observer [10], etc. Compared with other methods, ILO has a simple structure, easy design and less computational burden, which is more in line with engineering requirements. However, further improvement is needed to improve the convergence speed and accuracy. Compared with traditional FTC methods such as adaptive control and sliding mode control, prescribed performance control (PPC) can quantitatively design transient and steady-state performance a priori, and has a broader application prospect [11]. When there are faults or discontinuous references [12], PPC will cause control singularity problems due to unreachable original fixed performance, so its self-adaptive ability needs to be enhanced [13]. However, the current research rarely considers this problem, especially in the field of fault tolerant control. Inspired by the above results, the main contributions of this paper are as follows:

- A novel adaptive ILO (AILO) is proposed for actuator fault diagnosis, adding a more effective adaptive law design to deal with uncertainty and disturbance. The estimation speed and accuracy are improved compared to other methods.
- An adaptive finite time prescribed performance control (AFPPC) FTC method combining terminal sliding mode control is proposed, which can online adjust PPF boundaries. It solves the PPC singularity problem under uncertainty with reduced conservatism.
- We introduce an optimization algorithm to allocate actuators according to actuator faults. The overall energy consumption is reduced, and the faulty actuators can be optimally configured under remaining capacity and saturation constraints.

Remark 1: Compared with the ILO in [6], [9], the proposed AILO greatly improves the accuracy and speed of fault estimation by constructing a novel adaptive law. Compared with [14], [15], the proposed AFPPC adds the ability of adaptively adjusting PPF for faults and control references, avoiding the problem of unreachable performance under faults caused by traditional fixed PPF, and greatly expanding application range. Although a flexible PPF is designed in [13], the problem of discontinuous control reference is not considered.

II. SYSTEM DESCRIPTION AND PROBLEM STATEMENT

This paper uses quaternion $\boldsymbol{q}=[q_0, \boldsymbol{q_v}]^{\mathrm{T}}$ to describe the attitude. Let the target quaternion and target angular rate be $\boldsymbol{q}_d$ and $\boldsymbol{\omega}_d$, then $\boldsymbol{q}_e = \boldsymbol{q}_d^{-1} \otimes \boldsymbol{q}$ and $\boldsymbol{\omega}_e = \boldsymbol{\omega}$–$C_{bo}\boldsymbol{\omega}_d$ are the error quaternion and angular rate error, respectively. And $\otimes$ is the quaternion multiplication and $C_{bo} = (q_{e0}^2 - \boldsymbol{q}_{ev}^T\boldsymbol{q}_{ev})I_3 + 2\boldsymbol{q}_{ev}\boldsymbol{q}_{ev}^T - 2q_{e0}\boldsymbol{q}_{ev}^{\times}$ is the rotation matrix. The kinematics and dynamics model

*This work was supported in part by the National Natural Science Foundation of China under Grant 61427809

[1]Ze Yang, Baoqing Yang and Jie Ma are with the Department of Control Science and Engineering Harbin Institute of Technology, Harbin 150001, China mj_csc@163.com

[2]Ruihang Ji is with the Department of Electrical and Computer Engineering, National University of Singapore, 117576, Singapore jiruihang@nus.edu.sg (Corresponding author: Jie Ma.)

of an overactuated spacecraft can be described as:

$$\begin{aligned}&\dot{q}_{e0}=-\frac{1}{2}\boldsymbol{q}_e^{\mathrm{T}}\boldsymbol{\omega}_e,\dot{\boldsymbol{q}}_{ev}=\frac{1}{2}(\boldsymbol{q}_e^{\times}+q_{e0}I_3)\boldsymbol{\omega}_e\\&J_a\dot{\boldsymbol{\omega}}_e=-(\boldsymbol{\omega}_e+C_{bo}\boldsymbol{\omega}_d)^{\times}J_a(\boldsymbol{\omega}_e+C_{bo}\boldsymbol{\omega}_d)+\\&\qquad J_a(\boldsymbol{\omega}_e^{\times}C_{bo}\boldsymbol{\omega}_d-C_{bo}\dot{\boldsymbol{\omega}}_d)+(D_0+\Delta D)\boldsymbol{\lambda\tau}+\boldsymbol{\tau_d}\end{aligned}\tag{1}$$

in which $J_a=J_0+\Delta J\in\mathbb{R}^{3\times3}$ is the actual inertia, including nominal part J_0 and uncertain part ΔJ; $D_0+\Delta D\in\mathbb{R}^{3\times n}$ contains the nominal part D_0 and the uncertainty ΔD, representing the actuators configuration matrix; $\boldsymbol{\lambda}=\mathrm{diag}\{\lambda_1,\lambda_2,\cdots\lambda_n\}\in\mathbb{R}^{n\times n}$ denotes the health index matrix of actuators with $0\le\lambda_i\le1,i=1,\cdots,n$; $\boldsymbol{\tau}\in\mathbb{R}^n$ represents the control torque generated by n actuators; $\boldsymbol{\tau_d}$ denotes the unknown external disturbances. The skew symmetric matrix for any $\boldsymbol{c}=[c_1,c_2,c_3]^{\mathrm{T}}$ is denoted by $(\cdot)^{\times}$, and $\boldsymbol{c}^{\times}$ is defined as:

$$\boldsymbol{c}^{\times}=\begin{bmatrix}0&-c_3&c_2\\c_3&0&-c_1\\-c_2&c_1&0\end{bmatrix}\tag{2}$$

In this paper, multiplicative fault modeling $(D_0+\Delta D)\boldsymbol{\lambda\tau}$ is considered, given that it is mathematically equivalent to additive fault and facilitates subsequent control allocation design. Both actuator saturation and faults are considered, (1) can be rewritten as follows:

$$\begin{aligned}J_0\dot{\boldsymbol{\omega}}_e&=-\boldsymbol{\omega}^{\times}J_0\boldsymbol{\omega}+J_0\boldsymbol{\omega}_{\Delta}+D_0\lambda\mathrm{sat}(\boldsymbol{\tau})+\boldsymbol{d}\\&=-\boldsymbol{\omega}^{\times}J_0\boldsymbol{\omega}+J_0\boldsymbol{\omega}_{\Delta}+D_0\boldsymbol{E}(t)\mathrm{sat}(\boldsymbol{\tau})\\\boldsymbol{d}&=\bar{J}(-\boldsymbol{\omega}^{\times}J_a\boldsymbol{\omega}+\boldsymbol{u}_c+\boldsymbol{\tau}_d)+\boldsymbol{\tau}_d+\Delta D\boldsymbol{\lambda\tau}-\boldsymbol{\omega}^{\times}\Delta J\boldsymbol{\omega}\\\mathrm{sat}(\tau_i)&=\begin{cases}\tau_i&,if\ |\tau_i|\le\tau_{\max}\\\tau_{\max}\cdot\mathrm{sgn}(\tau_{\max})&,otherwise\end{cases}\end{aligned}\tag{3}$$

where $\boldsymbol{\omega}=\boldsymbol{\omega}_e+C_{bo}\boldsymbol{\omega}_d$, $\boldsymbol{\omega}_{\Delta}=\boldsymbol{\omega}_e^{\times}C_{bo}\boldsymbol{\omega}_d-C_{bo}\dot{\boldsymbol{\omega}}_d$, $\boldsymbol{E}(t)=\boldsymbol{\lambda}+\frac{\boldsymbol{d}}{D_0\boldsymbol{\tau}}=\mathrm{diag}\{e_1,e_2,\cdots e_n\}$ is the normalized health index and $\bar{J}=-(J_0+J_0(\Delta J)^{-1}J_0)^{-1}$; $\tau_{\max}$ is the maximum output torque of a single actuator; $\boldsymbol{u}_c=D_0\boldsymbol{E}(t)\boldsymbol{\tau}$ comes from the top-level controller to be designed.

The first step is to design the FD module to achieve faster and more accurate fault estimation under uncertainties and disturbances, laying a good foundation for FTC. Then we need to design a virtual control law based on adaptive PPC, which can adjust transient and steady-state performance constraints according to faults and commands, and avoid controller singularity. To resolve faults, saturation constraints, and accuracy requirements, a virtual control law must be mapped onto actuators through a novel allocation strategy.

III. ACTIVE FAULT TOLERANT CONTROL SCHEME DESIGN

Three components make up the AFTC scheme proposed in this paper: AILO-FD, AFPPC-FTC and online optimal allocation, as shown in Fig.1.

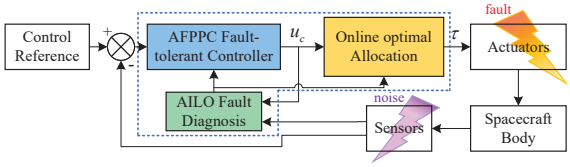

Fig. 1. Active Fault Tolerant Control Scheme.

A. AILO-based FD Mechanism

Inspired by the existing works in [6], [9], an improved AILO-based FD scheme is:

$$\begin{cases}J_0\dot{\hat{\boldsymbol{\omega}}}=-\hat{\boldsymbol{\omega}}^{\times}J_0\hat{\boldsymbol{\omega}}+D_0\hat{\boldsymbol{E}}(t)\boldsymbol{\tau}+\boldsymbol{k}_1(t)\tilde{\boldsymbol{\omega}}+\boldsymbol{k}_2(t)\mathrm{sgn}(\tilde{\boldsymbol{\omega}})\\\dot{\hat{\boldsymbol{E}}}(t)=k_3\hat{\boldsymbol{E}}(t-T)+\boldsymbol{k}_4(t)\tilde{\boldsymbol{\omega}}+k_5\tilde{\boldsymbol{\omega}}(t-T)\end{cases}\tag{4}$$

where $\hat{\boldsymbol{\omega}}$ and $\hat{\boldsymbol{E}}(t)$ are the estimations of $\boldsymbol{\omega}$ and $\boldsymbol{E}(t)$, respectively; $\tilde{\boldsymbol{\omega}}=\boldsymbol{\omega}-\hat{\boldsymbol{\omega}}$ is the angular rate estimation error; $\tilde{\boldsymbol{E}}=\boldsymbol{E}-\hat{\boldsymbol{E}}$ is the fault estimation error; $t-T$ represents the value before the time interval T; k_3,k_5 are positive-definite gain matrices; $k_1(t),k_2(t)$ and $k_4(t)$ are the adaptive control gain to be designed as:

$$\begin{aligned}\dot{k}_1(t)&=\begin{cases}\mu_1\left\|\tilde{\boldsymbol{\omega}}\right\|&,|\tilde{\boldsymbol{\omega}}|\le\delta_{\omega}\\0&,|\tilde{\boldsymbol{\omega}}|>\delta_{\omega}\end{cases},\dot{k}_4(t)=\begin{cases}\mu_4\left\|\tilde{\boldsymbol{\omega}}\right\|&,|\tilde{\boldsymbol{\omega}}|\le\delta_{\omega}\\0&,|\tilde{\boldsymbol{\omega}}|>\delta_{\omega}\end{cases}\\\dot{k}_2(t)&=\begin{cases}\mu_2\left\|\tilde{\boldsymbol{\omega}}\right\|\mathrm{sgn}(\left\|\tilde{\boldsymbol{\omega}}\right\|-\chi)&,k_2(t)>\bar{k}\\\gamma&,k_2(t)\le\bar{k}\end{cases}\end{aligned}\tag{5}$$

in which $\mu_1,\mu_2,\mu_4,\delta_{\omega},\bar{k},\chi$ and γ are positive constants that need to be chosen reasonably. There are fixed upper bound value $\bar{k}_1,\bar{k}_2,\bar{k}_4$ for setting the adaptive gain.

Assumption 1: The angular velocity $\boldsymbol{\omega}$ and its derivative $\dot{\boldsymbol{\omega}}$ are bounded. With a sufficiently small sampling time and known positive scalar σ, $\left\|\hat{\boldsymbol{\omega}}^{\times}J_0\hat{\boldsymbol{\omega}}-\boldsymbol{\omega}^{\times}J_0\boldsymbol{\omega}\right\|\le\sigma\left\|\tilde{\boldsymbol{\omega}}\right\|$ is satisfied. Besides, the normalized health index is bounded and satisfies $\left\|\boldsymbol{E}(t)-k_3\hat{\boldsymbol{E}}(t-T)\right\|\le\sigma_E$.

Proof: Choose a positive-definite Lyapunov function V_1 and deriving it gives:

$$\begin{aligned}V_1=&\frac{1}{2}\tilde{\boldsymbol{\omega}}^{\mathrm{T}}\tilde{\boldsymbol{\omega}}+\int_{t-T}^{t}\tilde{\boldsymbol{E}}^{\mathrm{T}}(\delta)\tilde{\boldsymbol{E}}(\delta)d\delta+\frac{1}{2\mu_2}(k_2-\bar{k}_2)^2+\\&\frac{1}{2\mu_1}(k_1-\bar{k}_1)^2+\frac{1}{2\mu_4}(k_4-\bar{k}_4)^2\\\dot{V}_1=&\tilde{\boldsymbol{\omega}}^{\mathrm{T}}\dot{\tilde{\boldsymbol{\omega}}}+\tilde{\boldsymbol{E}}^{\mathrm{T}}(t)\tilde{\boldsymbol{E}}(t)-\tilde{\boldsymbol{E}}^{\mathrm{T}}(t-T)\tilde{\boldsymbol{E}}(t-T)+\\&(k_2-\bar{k}_2)\frac{\dot{k}_2}{\mu_2}+(k_1-\bar{k}_1)\frac{\dot{k}_1}{\mu_1}+(k_4-\bar{k}_4)\frac{\dot{k}_4}{\mu_4}\end{aligned}\tag{6}$$

By combining (3) and (4), the observer error can be obtained as $\dot{\tilde{\boldsymbol{E}}}(t)=k_3\tilde{\boldsymbol{E}}(t-T)-k_4(t)\tilde{\boldsymbol{\omega}}-k_5\tilde{\boldsymbol{\omega}}(t-T)+\boldsymbol{h}(t),\dot{\tilde{\boldsymbol{\omega}}}=\boldsymbol{\omega}^{\times}J_0\boldsymbol{\omega}-\hat{\boldsymbol{\omega}}^{\times}J_0\hat{\boldsymbol{\omega}}+\tilde{\boldsymbol{E}}_t-k_1\tilde{\boldsymbol{\omega}}_t-k_2\mathrm{sgn}(\tilde{\boldsymbol{\omega}}_t)$. Where $\boldsymbol{h}(t)=\boldsymbol{E}(t)-k_3\boldsymbol{E}(t-T)$. To simplify the representation, $(\cdot)(t)$ is represented by $(\cdot)_t$. We can get:

$$\begin{aligned}\tilde{\boldsymbol{E}}_t^{\mathrm{T}}\tilde{\boldsymbol{E}}_t=&k_3^2\tilde{\boldsymbol{E}}_{t-T}^{\mathrm{T}}\tilde{\boldsymbol{E}}_{t-T}-2k_4k_3\tilde{\boldsymbol{E}}_{t-T}^{\mathrm{T}}\tilde{\boldsymbol{\omega}}-2k_5k_3\tilde{\boldsymbol{E}}_{t-T}^{\mathrm{T}}\tilde{\boldsymbol{\omega}}_{t-T}\\&+2k_3\tilde{\boldsymbol{E}}_{t-T}^{\mathrm{T}}\boldsymbol{h}_t+k_4^2\tilde{\boldsymbol{\omega}}_t^{\mathrm{T}}\tilde{\boldsymbol{\omega}}_t+2k_4k_5\tilde{\boldsymbol{\omega}}_t^{\mathrm{T}}\tilde{\boldsymbol{\omega}}_{t-T}-\\&2k_4\tilde{\boldsymbol{\omega}}_t^{\mathrm{T}}\boldsymbol{h}_t-2k_5\tilde{\boldsymbol{\omega}}_{t-T}^{\mathrm{T}}\boldsymbol{h}_t+k_5^2\tilde{\boldsymbol{\omega}}_{t-T}^{\mathrm{T}}\tilde{\boldsymbol{\omega}}_{t-T}+\boldsymbol{h}_t^{\mathrm{T}}\boldsymbol{h}_t\end{aligned}\tag{7}$$

By Young's inequality, we can conclude that

$$\begin{aligned}
&2k_4k_3\tilde{E}_{t-T}^{\mathrm{T}}\bar{\omega}\le a_1k_3^2\tilde{E}_{t-T}^{\mathrm{T}}\tilde{E}_{t-T}+\tfrac{k_4^2}{a_1}\bar{\omega}^{\mathrm{T}}\bar{\omega}\\
&2k_5k_3\tilde{E}_{t-T}^{T}\tilde{\omega}_{t-T}\le a_2k_3^2\tilde{E}_{t-T}^{\mathrm{T}}\tilde{E}_{t-T}+\tfrac{k_5^2}{a_2}\tilde{\omega}_{t-T}^{\mathrm{T}}\bar{\omega}_{t-T}\\
&2k_3\tilde{E}_{t-T}^{\mathrm{T}}h_t\le a_3k_3^2\tilde{E}_{t-T}^{\mathrm{T}}\tilde{E}_{t-T}+\tfrac{1}{a_3}h_t^{\mathrm{T}}h_t\\
&2k_4k_5\tilde{\omega}_t^{T}\tilde{\omega}_{t-T}\le a_4k_5^2\tilde{\omega}_t^{\mathrm{T}}\tilde{\omega}_t+\tfrac{k_4^2}{a_4}\tilde{\omega}_{t-T}^{\mathrm{T}}\tilde{\omega}_{t-T}\\
&2k_4\tilde{\omega}_t^{\mathrm{T}}h_t\le a_5k_4^2\tilde{\omega}_t^{\mathrm{T}}\tilde{\omega}_t+\tfrac{1}{a_5}h_t^{\mathrm{T}}h_t\\
&2k_5\tilde{\omega}_{t-T}^{T}h_t\le a_6k_5^2\tilde{\omega}_{t-T}^{\mathrm{T}}\tilde{\omega}_{t-T}+\tfrac{1}{a_6}h_t^{T}h_t\\
&\tilde{\omega}_t^{\mathrm{T}}\tilde{E}_t\le\tfrac{a_7}{2}\tilde{\omega}_t^{\mathrm{T}}\tilde{\omega}_t+\tfrac{1}{2a_7}\tilde{E}_t^{\mathrm{T}}\tilde{E}_t
\end{aligned}\tag{8}$$

There exists a constant ζ such that (6) can be further organized as follows:

$$\begin{aligned}
\dot{V}_1\le&[\sigma+\frac{a_7}{2}-\lambda_{\min}(k_1)+1+(1+\zeta+\frac{1}{2a_7})b_2]\|\tilde{\boldsymbol{\omega}}_t\|^2-\zeta\left\|\tilde{\boldsymbol{E}}_t\right\|^2\\
&+[(1+\zeta+\frac{1}{2a_7})b_1-1]\left\|\tilde{\boldsymbol{E}}_{t-T}\right\|^2+[(1+\zeta+\frac{1}{2a_7})b_3-1]\\
&\|\tilde{\boldsymbol{\omega}}_{t-T}\|^2-k_2\|\tilde{\boldsymbol{\omega}}_t\|+(1+\zeta+\frac{1}{2a_7})b_4\|\boldsymbol{h}_t\|^2+(k_2-\bar{k}_2)\frac{\dot{k}_2}{\mu_2}\\
&+(k_1-\bar{k}_1)\frac{\dot{k}_1}{\mu_1}+(k_4-\bar{k}_4)\frac{\dot{k}_4}{\mu_4}
\end{aligned}\tag{9}$$

where $b_1=(1+a_1+a_2+a_3)k_3^2, b_2=(1+\frac{1}{a_1}+a_4+a_5)k_4^2, b_3=(1+\frac{1}{a_2}+\frac{1}{a_4}+a_6)k_5^2, b_4=1+\frac{1}{a_3}+\frac{1}{a_5}+\frac{1}{a_6}$. If μ_1,μ_2,μ_4 are properly selected so that the following relationship holds:

$$\begin{aligned}
&\eta+\tfrac{a_7}{2}-\lambda_{\min}(k_1)+1+(1+\zeta+\tfrac{1}{2a_7})b_2>0\\
&(1+\zeta+\tfrac{1}{2a_7})b_1-1<0\ ,\ (1+\zeta+\tfrac{1}{2a_7})b_3-1<0
\end{aligned}\tag{10}$$

Then the stability of V_1 is satisfied, and the proof is completed. Increasing μ_1,μ_2,μ_4,γ can increase the estimation rapidity and the overshoot, while reducing accuracy; reducing δ_ω,χ can improve the accuracy. ■

B. AFPPC Fault Tolerant Controller

Traditional PPC makes the system error satisfy $\rho_1(t)<q_{ev}(t)<\rho_2(t)$, but $\rho_1(t),\rho_2(t)$ is fixed. However, actuator faults will degrade the control performance, making the initial given performance unreachable. In addition, the control reference is not necessarily continuous, which also limits the implementation of traditional PPC [16]. In order to solve the above problems, this paper proposes a novel adaptive finite time prescribed performance function (AFPPF) as follows:

$$\begin{aligned}
&\rho_1(t)=[\mathrm{sgn}(q_{ev}(0))-\delta_1]\rho_k(t)-\rho_\infty\mathrm{sgn}(q_{ev}(0))\\
&\rho_2(t)=[\mathrm{sgn}(q_{ev}(0))+\delta_2]\rho_k(t)-\rho_\infty\mathrm{sgn}(q_{ev}(0))\\
&\rho_k(t)=\begin{cases}(\rho_{k0}^{\tau}-\tau\lambda t)^{1/\tau}+\rho_{k\infty}, t\in[0,t_f]\\ \rho_{k\infty}\qquad\qquad\quad, t\in[t_f,\infty]\end{cases}, k=1,2,\dots
\end{aligned}\tag{11}$$

among them, ρ_1 and ρ_2 are the performance lower bound and upper bound; $\rho_{k0},\rho_{k\infty}>0$; $t_f=\frac{\rho_{k0}^{\tau}}{\tau\lambda}$ is the convergence time chosen by the designer. And k records the number of times the PPF re-converges when the system runs to t_f. In order to enable the PPF to be adaptively updated online according to faults and control references, k records the number of times the performance function re-converges when the control system runs to time t_f. When the control reference and fault change, $k=k+1$, and update the parameters according to the following method:

$$\begin{aligned}
&\rho_{k0}=\eta\cdot\max(q_{ev,i}), i=1,2,3\\
&t_f=\max\left[\sqrt{\kappa\cdot\frac{\pi}{180}\cdot\frac{4\theta_{e,i}J_{ii}}{\tau_{\max}\hat{E}_i}}\right], i=1,2,3
\end{aligned}\tag{12}$$

where J_{ii} is the inertia moment of the i-th axis; $\theta_{e,i}$ is the Euler angle error under the new control reference, and $q_{ev,i}$ is the error quaternion converted from it; $\eta,\kappa>1$ are gain margins to increase robustness. Then we introduce error transformation function as (13) to transform the original system with the constrained tracking error into an equivalent unconstrained one.

$$\boldsymbol{\varepsilon}=\ln\left(\frac{\boldsymbol{q}_{ev}-\rho_1(t)}{\rho_2(t)-\boldsymbol{q}_{ev}}\right)\tag{13}$$

where $\boldsymbol{\varepsilon}$ is the transformed error, and we can get $\dot{\boldsymbol{\varepsilon}}$ as:

$$\dot{\boldsymbol{\varepsilon}}=\frac{\rho_2-\rho_1}{(\rho_2-\boldsymbol{q}_{ev})(\boldsymbol{q}_{ev}-\rho_1)}\left[\dot{\boldsymbol{q}}_{ev}+\frac{\rho_1\dot{\rho}_2-\dot{\rho}_1\rho_2+(\dot{\rho}_1-\dot{\rho}_2)\boldsymbol{q}_{ev}}{\rho_2-\rho_1}\right]\tag{14}$$

Consider a fast terminal sliding surface $\boldsymbol{s}\in R^{3\times1}$ as $\boldsymbol{s}=\boldsymbol{\omega}_e+\beta_1\boldsymbol{\varepsilon}+\beta_2 sig(\boldsymbol{\varepsilon})^r$, where $\beta_1,\beta_2>0, 0<r<1, sig(\boldsymbol{\varepsilon})^r=\mathrm{diag}(\mathrm{sgn}(\varepsilon_i)|\varepsilon_i|^r)$. The time derivative of $\boldsymbol{s}$ using (3) and (14) yields:

$$\begin{aligned}
J_0\dot{\boldsymbol{s}}&=J_0(\beta_1\dot{\boldsymbol{\varepsilon}}+\dot{\boldsymbol{\omega}}_e+\beta_2r\dot{\boldsymbol{\varepsilon}}G_e)\\
&=-\boldsymbol{\omega}^{\times}J_0\boldsymbol{\omega}+D_0E(t)\boldsymbol{\tau}+J_0\beta_1\dot{\boldsymbol{\varepsilon}}+J_0\beta_2r\dot{\boldsymbol{\varepsilon}}G_e
\end{aligned}\tag{15}$$

where $G_e=\mathrm{diag}(|\varepsilon_i|^{r-1}),\ \ i=1,2,3$. Following is the proposed fast terminal sliding mode control (FTSMC) law:

$$\boldsymbol{u}_c=-\boldsymbol{\omega}^{\times}J_0\boldsymbol{\omega}-J_0\beta_1\dot{\boldsymbol{\varepsilon}}-J_0\beta_2rG_e\dot{\boldsymbol{\varepsilon}}-\beta_3\boldsymbol{s}-\beta_4sig(\boldsymbol{s})^r\tag{16}$$

where β_3,β_4 are positive-definite gain matrices; and the actuator torque can be obtained by $\boldsymbol{\tau}=[D_0\hat{\boldsymbol{E}}(t)]^{\dagger}\boldsymbol{u}_c$.

Theorem 1: Consider the system (3) and the sliding mode surface $\boldsymbol{s}$. The proposed AFPPC fault tolerant controller (AFPPC-FTC) (16) can guarantee $\boldsymbol{s}$ and $\boldsymbol{q}_e$ converge in finite time. In addition, the proposed strategy ensures that the system is always under prescribed performance constraints (11). The stability and performance of FTC can be satisfied by properly selecting $\beta_1,\beta_2,\beta_3,\beta_4$ so that the following inequality holds.

Proof: Firstly, we demonstrate the stability of the sliding surface $\boldsymbol{s}$, and the Lyapunov function is selected as $V_1=\frac{1}{2}\boldsymbol{s}^{\mathrm{T}}J_0\boldsymbol{s}$, and its derivative $\dot{V}_1$ is:

$$\dot{V}_1=\boldsymbol{s}^{\mathrm{T}}J_0\dot{\boldsymbol{s}}=\boldsymbol{s}^{\mathrm{T}}\left[-\boldsymbol{\omega}^{\times}J_0\boldsymbol{\omega}+D_0\boldsymbol{E}\boldsymbol{\tau}+\beta_1J_0\dot{\boldsymbol{\varepsilon}}+\beta_2J_0r\dot{\boldsymbol{\varepsilon}}G_e\right]\tag{17}$$

Substituting $\boldsymbol{u}_c$ from (16) into (17) gives:

$$\begin{aligned}
\dot{V}_1&=\boldsymbol{s}^{\mathrm{T}}[D_0(\boldsymbol{E}(t)-\hat{\boldsymbol{E}}(t))\boldsymbol{\tau}-\beta_3\boldsymbol{s}-\beta_4sig(\boldsymbol{s})^r]\\
&\le-\beta_3\|\boldsymbol{s}\|^2-\|\boldsymbol{s}\|^{\mathrm{T}}\beta_4\|\boldsymbol{s}\|^r+\zeta\|\boldsymbol{s}\|\\
&\le-(\|\boldsymbol{s}\|^{\mathrm{T}}\beta_4\|\boldsymbol{s}\|^{r-1}-\zeta)\|\boldsymbol{s}\|\le-\sum_{i=1}^{3}K_i(\|s_i\|^2)^{\frac{r+1}{2}}
\end{aligned}\tag{18}$$

where $\left\|D_0(\boldsymbol{E}(t)-\hat{\boldsymbol{E}}(t))\boldsymbol{\tau}\right\|\le\zeta$; K_i is the diagonal element of the matrix $\|\boldsymbol{s}\|^{\mathrm{T}}\beta_4\|\boldsymbol{s}\|^{r-1}-\zeta$. According to $\beta_4>$

$\zeta/\|\boldsymbol{s}\|^r$, design the appropriate β_3, β_4 to ensure negative definiteness. Then we can get:

$$\dot{V}_1 \leq -\min\{K_i\} 2^{\frac{r+1}{2}} V_1^{\frac{r+1}{2}} \tag{19}$$

Let $\alpha = \frac{r+1}{2}$, then the system can reach $s=0$ within a finite time $T \leq V_1^{1-\alpha}/\min\{K_i\}2^{\frac{r+1}{2}}(1-\alpha)$.

We further prove that the stability of $\boldsymbol{q}_e$ as $\boldsymbol{s}$ approaches 0. Consider the following new Lyapunov function $V_2 = \frac{1}{2}\boldsymbol{\varepsilon}^{\mathrm{T}}\boldsymbol{\varepsilon}$. As $\boldsymbol{s}\to 0$, we have $\boldsymbol{\omega} = -\beta_1\boldsymbol{\varepsilon} - \beta_2 sig(\boldsymbol{\varepsilon})^r$, and substitute (14) to get:

$$\dot{V}_2 = \boldsymbol{\varepsilon}^T\dot{\boldsymbol{\varepsilon}} = -\boldsymbol{\varepsilon}^T A\beta_1 Q\boldsymbol{\varepsilon} - \boldsymbol{\varepsilon}^T A\beta_2 Q sig(\boldsymbol{\varepsilon})^r + \boldsymbol{\varepsilon}^T AB \tag{20}$$

where $A = \frac{\rho_2-\rho_1}{(\rho_2-q_{ev})(q_{ev}-\rho_d)}$, $B = \frac{\rho_1\dot{\rho}_2 - \dot{\rho}_1\rho_2 + (\dot{\rho}_1-\dot{\rho}_2)q_{ev}}{\rho_2-\rho_1}$ and $Q = \frac{1}{2}(q_v^{\times} + q_0 I_3)$. Furthermore, $\rho_2 - \rho_1$ is positive and bounded. Due to the nature of $\rho(t)$, it can be deduced that $A \cdot B$ is positive definite. It is not difficult to see that Q determines whether the first two terms in (20) are positive definite. The principal minor values of Q are $q_0, q_0^2 + q_3^2, 0.5q_0$. When the system enters a steady state, $\boldsymbol{q}_{ev}$ will will converge to a neighborhood of 0. Therefore, by proving $\dot{V}_1 < 0$ and $\dot{V}_2 < 0$, it is certain that the system will converge in a finite time. ■

C. Online Fault Tolerant Optimal Allocation

For overactuated systems, the control law generated by the controller needs to be assigned to actuators. However, pseudo-inverse method cannot handle optimal allocation under additional constraints. This section introduces second-order cone programming (SOCP) [15] to allocate actuators. Considering that $\hat{E}(t)$ from FD cannot be completely accurate, the relationship between u_c and τ is $u_c = D_0(I_n - E_\Delta)\hat{E}\tau$, where $E_\Delta = diag(E_{\delta 1}, E_{\delta 2}, \cdots, E_{\delta n})$ is the estimation error. Further considering actuator faults and capability constraints, the optimization problem involves uncertainties is as follows:

$$\tau = \arg \min_{\|\tau_i\| \leq \hat{E}_i \tau_{\max}} \max^{\|E_\Delta\| \leq \bar{E}} \{\tau^{\mathrm{T}} P\tau + h\left\|D_0(I_n - E_\Delta)\hat{E}\tau - u_c\right\|^2\} \tag{21}$$

where the constant $h > 0$, $\bar{E}$ is known positive scalar, and P is a positive definite weight matrix. For the SOCP in (21), the second term represents the process of minimizing the worst-case residuals to obtain the optimal $\boldsymbol{u}_c$. In this way, the worst residual to control allocation is able to establish some robustness against the fault estimation error. In addition, SOCP represents a secondary objective aimed at minimizing energy consumption, as embodied in the first term.

$$\tau = \arg \min_{\|\tau_i\| \leq \hat{E}_i \tau_{\max}} \{\tau^{\mathrm{T}} P\tau + h(\left\|D_0(I_n - E_\Delta)\hat{E}\tau - u_c\right\| + \bar{E})^2\} \tag{22}$$

SOCP formulation can be solved as follows to obtain the solution to the aforementioned problem:

$$\min_{\tau, y_k} y_1, \ s.t. \begin{cases} \|col(y_2, y_3)\| \leq y_1 \\ \left\|P^{1/2}\tau\right\| \leq y_2 \\ \left\|D_0(I_n - E_\Delta)\hat{E}\tau - u_c\right\| \leq \frac{y_3}{\sqrt{h}} - \bar{E} \\ \|\tau\| \leq \hat{E}_i \tau_{\max} \end{cases} \tag{23}$$

where $y_i, i = 1, 2, 3, 4$ are intermediate variables, and $col(y_2, y_3)$ is a column vector composed of y_2 and y_3. The above problems can be solved by using numerical optimization software to obtain the optimal τ.

IV. SIMULATION

To verify the effectiveness of the proposed AFTC scheme, numerical experiments based on fixed-step Runge–Kutta ($T = 0.01s$) are performed for a rigid spacecraft with the inertia and disturbances taken as:

$$\begin{aligned} J_0 &= \begin{bmatrix} 43 & 0.3 & 1.2 \\ 0.3 & 52 & -0.5 \\ 1.2 & -0.5 & 40 \end{bmatrix} kg{\cdot}m^2, \Delta J = 0.1J_0 \\ \tau_{d\phi} &= 10^{-3}[0.6\cos(0.05t)\sin(0.11t)]N{\cdot}m \\ \tau_{d\theta} &= 10^{-3}[1+3\sin(0.06t)]N{\cdot}m \\ \tau_{d\psi} &= 10^{-3}[1+\cos(0.07t)\cos(0.21t)]N{\cdot}m \end{aligned} \tag{24}$$

The angular rate gyro noise is selected as white noise with a variance of 0.001 degrees. And the actuators configuration matrix is selected as:

$$D_0 = \begin{bmatrix} 1 & 0 & 0 & 1/\sqrt{3} \\ 0 & 1 & 0 & 1/\sqrt{3} \\ 0 & 0 & 1 & 1/\sqrt{3} \end{bmatrix}, \Delta D = 0.01D_0 \tag{25}$$

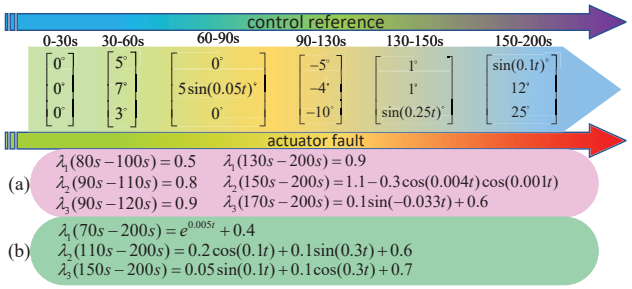

Fig. 2. Actuator Faults Scenario and Control Reference setting.

Four actuators are installed in a three-orthogonal and one-oblique configuration and the $4th$ redundant actuator is activated after the first detection of fault. In order to verify the proposed AILO algorithm, two scenarios as shown in Fig.2 are set up to verify its ability to track abrupt faults and fast time-varying faults. Considering that in practice the fault will not change as fast as (b), the AFPPC verification will be based on (a). Fig.2 shows the Euler angle time sequences for verifying AFPPF's adaptive adjustment ability.

As shown in Fig.3, comparisons are made in two fault scenarios. Among them, the above is the proposed AILO, and the below is the traditional ILO [6], [9]. It is easy to see that the improved AILO proposed in this paper not only improves the estimation accuracy, but also has a significantly faster speed, which can better meet the real-time requirement and directly improve the AFTC performance. In terms of algorithm complexity, the simulation process takes 3.5411s for AILO and 3.2365s for ILO, which shows that the improved AILO slightly

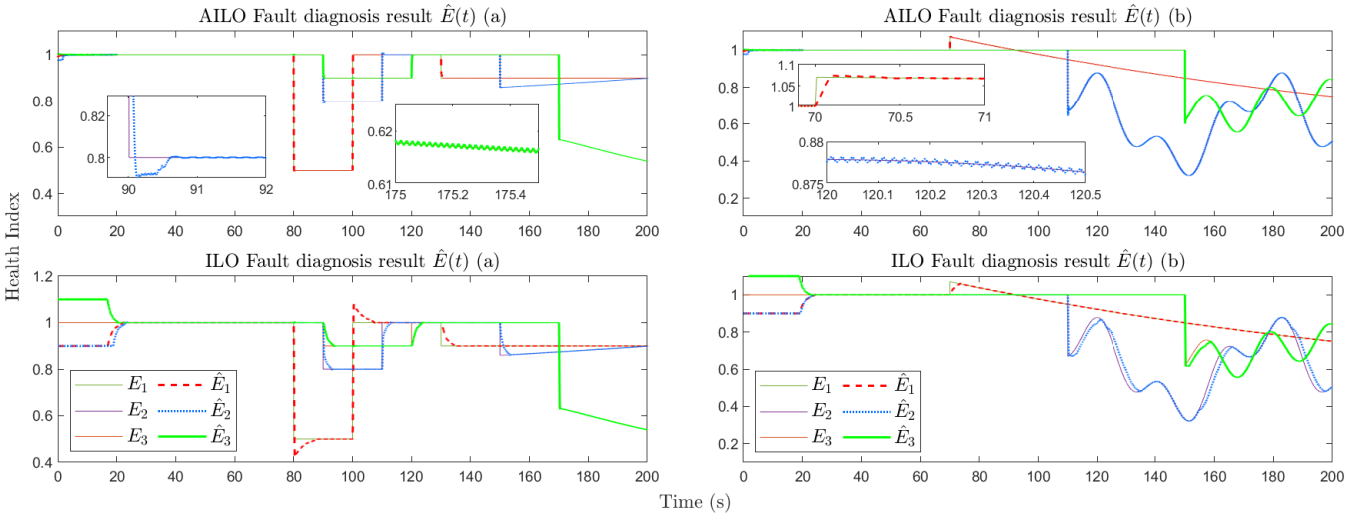

Fig. 3. Actuator Fault Diagnostic Result $\hat{E}(t)$ Based on AILO and ILO.

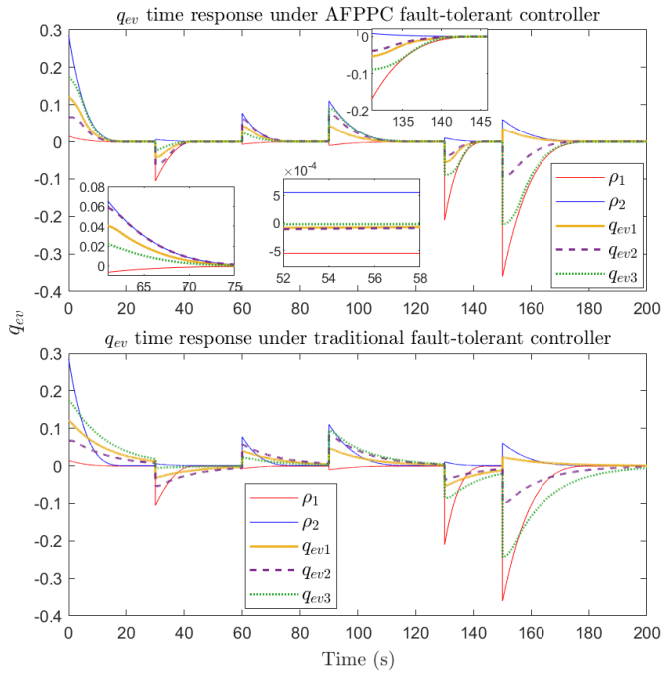

Fig. 4. Time Response of q_{ev} with performance constraints.

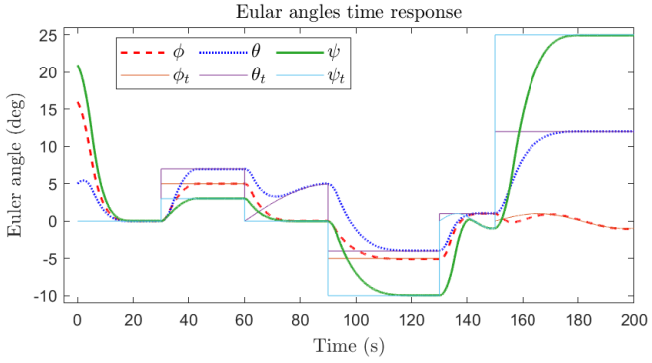

Fig. 5. Euler angle Time Response under AFPPC-FTC.

TABLE I
Comparison of estimation RMSE of AILO and ILO

Method	Scenario	RMSE E_1	RMSE E_2	RMSE E_3
AILO	(a)	**3.69e − 05**	**2.43e − 04**	**1.49e − 04**
	(b)	**1.01e − 04**	**2.63e − 04**	**6.11e − 05**
ILO	(a)	0.0084	0.009	0.0093
	(b)	0.0107	0.0092	0.0091

increases the complexity of the algorithm. Table I shows the comparison of the RMSE values of the two methods under different fault conditions. It can be seen that the improved AILO with adaptive law has higher accuracy.

Based on the AILO-FD, the accurate diagnosis results of actuators are given, and then the proposed AFPPC-FTC generates virtual control law according to the health status of the actuators to offset the faults.

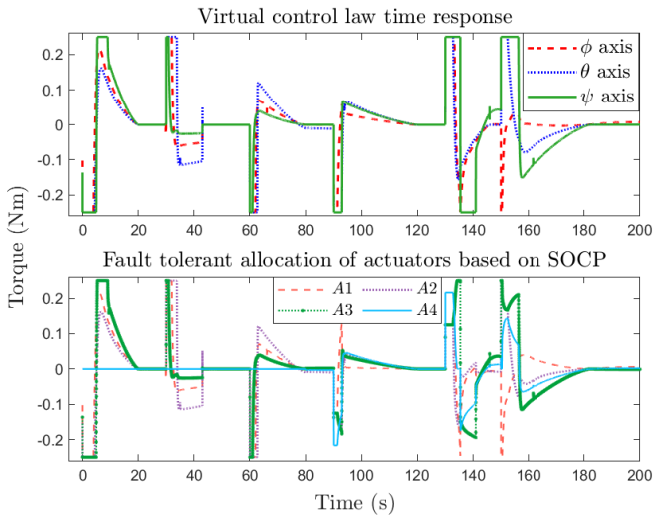

Fig. 6. Virtual Control Law and SOCP Fault Tolerant Allocation.

Fig.4 illustrates $\boldsymbol{q}_{ev}$ output responses based on AF-

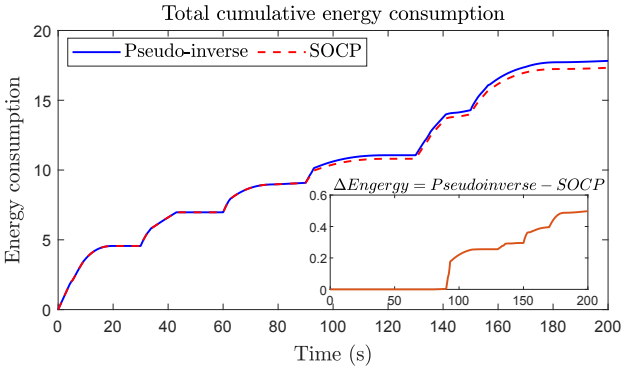

Fig. 7. Comparison of Energy Consumption.

PPC and traditional FTSMC respectively. Traditional controllers do not have prescribed performance, and therefore cannot be quantitatively designed, resulting in the inability to fully utilize the capabilities of the system. PPC can directly correlate transient and steady-state performance with controller parameters, reducing conservatism. However, the traditional PPC cannot handle discontinuous control commands, and the initial parameters are fixed, which limits the application.

The improved AFPPC can adaptively adjust the performance constraint and dynamically update it according to the control command and the health status of the actuator. In addition, it also solved the problem that traditional PPC cannot be applied to non-continuous control sequences. Fig.5 demonstrates the Euler angles time response and the corresponding commands more clearly and intuitively. With the proposed AFTC scheme, the system can still achieve prescribed accuracy and transient performance. Compared with the traditional PPC, the improved AFPPC hardly increases the computational complexity.

Next, the actuator saturation is considered in simulation, $\tau_{\max}$ of actuators is set as $0.25Nm$. As shown in Fig.6, the virtual control law u_c generated by AFPPC-FTC and the actuator torque allocated online by SOCP are given respectively. As a comparison, the SOCP can not only achieve precise allocation, but also find the optimal solution within the limit constraints according to the health status of actuators. To examine the effectiveness, we use $\int_0^t \|\tau(\delta)\|^2 d\delta$ as an indicator to evaluate energy consumption. It is not difficult to see from Fig.7 that the SOCP method mentioned in (21-23) is also slightly better than the pseudo-inverse allocation.

V. CONCLUSIONS

In this study, an AFTC scheme applied to attitude maneuvers is proposed. Among them, AILO has improved the adaptive law with higher estimation accuracy and convergence speed. Meanwhile, the robustness to uncertainty and disturbance is guaranteed. AFPPC-FTC can adaptively adjust the transient and steady state performance according to the faults and commands. There is no need to repeatedly design controller parameters, avoid singularity in PPC caused by unreachable performance, and reduce the conservatism. The SOCP based online optimal allocation algorithm can realize the fault tolerant allocation of actuators with better performance under the constraints of saturation and faults. In addition, numerical simulations are used to demonstrate the effectiveness and superiority of the proposed method. Moreover, how to handle faults when the system enters a steady state and without new discontinuous reference needs to be further studied in the future.

References

[1] Hasan M N, Haris M, Qin S, "Fault-tolerant spacecraft attitude control: A critical assessment," Progress in Aerospace Sciences, vol. 130, pp. 100806, 2022.

[2] Han Y, Biggs J D, Cui N, "Adaptive fault-tolerant control of spacecraft attitude dynamics with actuator failures,"Journal of Guidance, Control, and Dynamics, vol. 38, no. 10, pp. 2033-2042, 2015.

[3] Yin S, Xiao B, Ding S X, et al, "A review on recent development of spacecraft attitude fault tolerant control system," IEEE Transactions on Industrial Electronics, vol. 63, no. 5, pp. 3311-3320, 2016.

[4] Jiang J, Yu X, "Fault-tolerant control systems: A comparative study between active and passive approaches," Annual Reviews in control, vol. 36, no. 1, pp. 60-72, 2012.

[5] Ji R, Ge S S, Li D, "Saturation-tolerant prescribed control for nonlinear systems with unknown control directions and external disturbances," IEEE Transactions on Cybernetics, 2023.

[6] Zhang C, Wang J, Zhang D, et al, "Learning observer based and event-triggered control to spacecraft against actuator faults[J]. Aerospace Science and Technology, vol. 78, pp. 522-530, 2018.

[7] Ran D, Chen X, de Ruiter A, et al, "Adaptive extended-state observer-based fault tolerant attitude control for spacecraft with reaction wheels," Acta Astronautica, vol. 145, pp. 501-514, 2018.

[8] Yang Z, Ma J, Ji R, Yang B, Fan X, "IAR-STSCKF-based fault diagnosis and reconstruction for spacecraft attitude control systems," IEEE Transactions on Instrumentation and Measurement, vol. 71, pp. 1-12, 2022.

[9] Hu Q, Zhang X, Niu G, "Observer-based fault tolerant control and experimental verification for rigid spacecraft," Aerospace Science and Technology, vol. 92, pp. 373-386, 2019.

[10] Zhang X, Zong Q, Tian B, et al, "Finite-time fault estimation and fault-tolerant control for rigid spacecraft," Journal of Aerospace Engineering, vol. 31, no. 6, pp. 04018091, 2018.

[11] Wei C, Chen Q, Liu J, et al, "An overview of prescribed performance control and its application to spacecraft attitude system," Proceedings of the Institution of Mechanical Engineers, vol. 235, no. 4, pp. 435-447, 2021.

[12] Fotiadis F, Rovithakis G A, "Prescribed performance control for discontinuous output reference tracking," IEEE Transactions on Automatic Control, vol. 66, no. 9, pp. 4409-4416, 2020.

[13] Bu X, Jiang B, Lei H, "Nonfragile quantitative prescribed performance control of waverider vehicles with actuator saturation," IEEE Transactions on Aerospace and Electronic Systems, vol. 58, no. 4, pp. 3538-3548, 2022.

[14] Gao S, Liu X, Jing Y, et al, "A novel finite-time prescribed performance control scheme for spacecraft attitude tracking," Aerospace Science and Technology, vol. 118, pp. 107044, 2021.

[15] Yin Z, Suleman A, Luo J, et al, "Appointed-time prescribed performance attitude tracking control via double performance functions," Aerospace Science and Technology, vol. 93, pp. 105337, 2019.

[16] Shen Q, Wang D, Zhu S, et al, "Robust control allocation for spacecraft attitude tracking under actuator faults," IEEE Transactions on Control Systems Technology, vol. 25, no. 3, pp. 1068-1075, 2016.